Supplementary Information

Ultrasmooth Perovskite Films Formed toward Highly Efficient Inverted Planar Heterojunction Solar Cells by Micro-flowing Anti-solvent Deposition in Air

Bin Xia [†a], *Zhaoxin Wu* [†*a], *Hua Dong* [a], *Jun Xi* [a], *Wen Wu* [a], *Ting Lei* [a], *Kai Xi* [c], *Fang Yuan* [a], *Bo Jiao* [a], *Lixin Xiao* [b], *Qihuang Gong* [b], *and Xun Hou* [a]

[a] Key Laboratory of Photonics Technology for information,

Key Laboratory for Physical Electronics and Devices of the Ministry of Education,

School of Electronic and Information Engineering,

Xi'an Jiaotong University, Xi'an, 710049, P. R. China

Tel: +86-29-82664867

E-mail: zhaoxinwu@mail.xjtu.edu.cn

[b] State Key Laboratory for Mesoscopic Physics and Department of Physics,

Peking University, Beijing, 100871, P. R. China

[c] Department of Materials Science and Metallurgy,

University of Cambridge, Cambridge, CB2 3QZ, UK

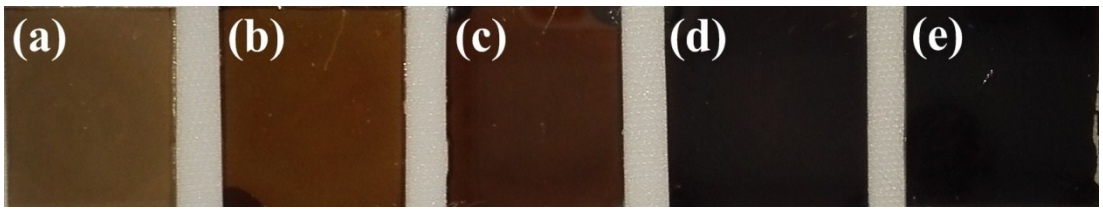

Fig. S1 Perovskite films by different $CH_3NH_3PbI_3$ concentration of (a) 15%, (b) 25%, (c) 35%, (d) 45%, and (e) 55%.

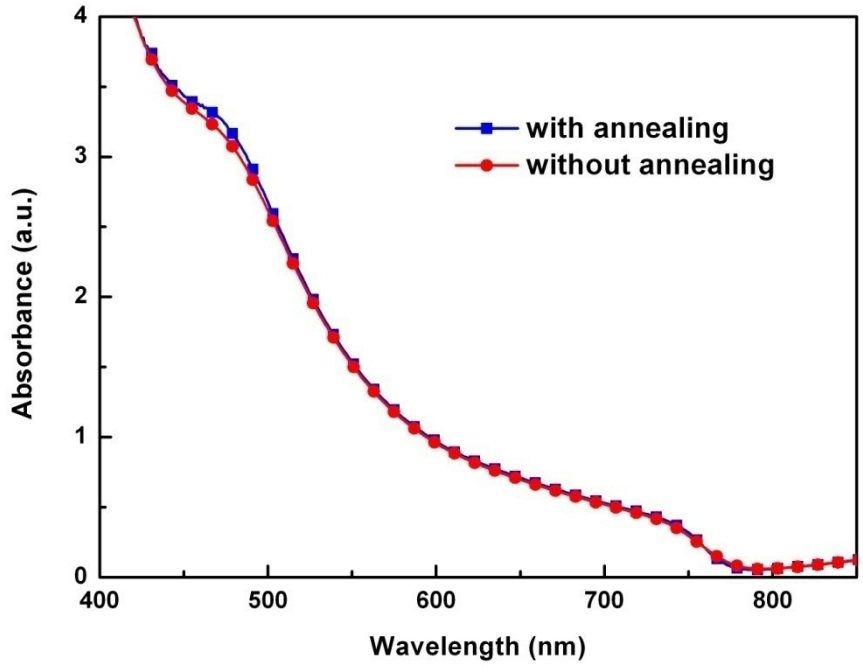

Fig. S2 Absorption spectra of perovskite films prepared by MAD with and without annealing procedure.

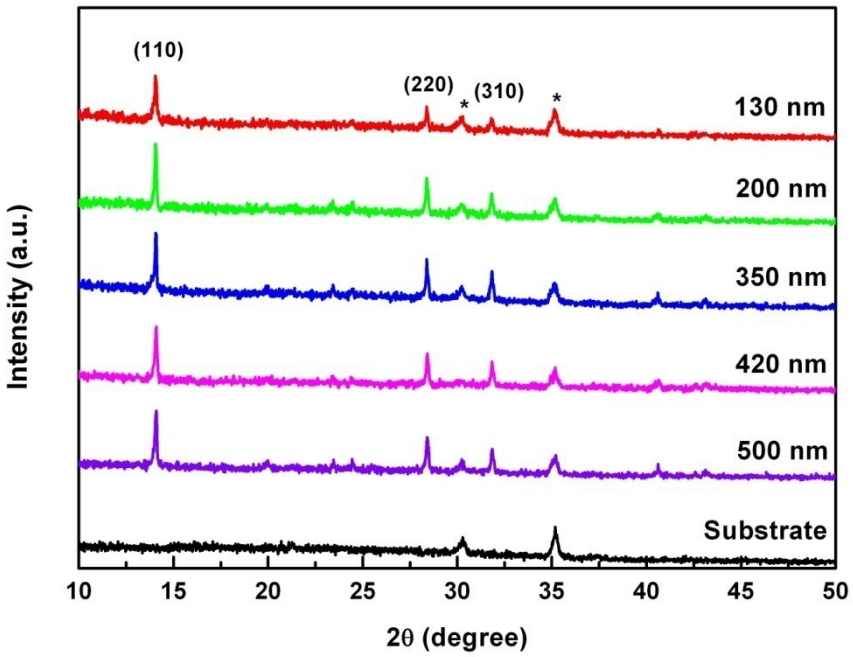

Fig. S3 XRD patterns of perovskite films with different thicknesses formed by different $CH_3NH_3PbI_3$/DMF solution concentrations. 130 nm, 200 nm, 350 nm, 420 nm and 500 nm film thickness corresponded to 15wt%, 25wt%, 35wt%, 45wt% and 55wt% $CH_3NH_3PbI_3$/DMF concentrations, respectively. (110), (220), and (310) represent diffraction of main crystal faces in tetragonal perovskite phase and asterisks represent diffraction peak of substrate.

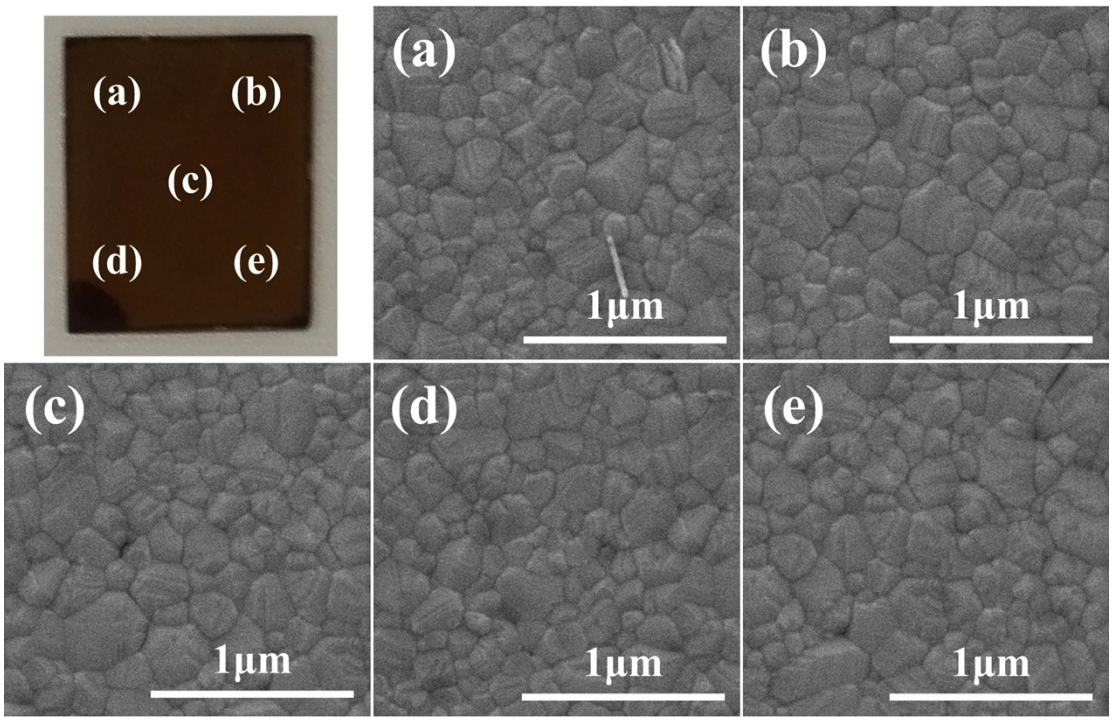

Fig. S4 SEM images of perovskite film at five areas (from area (a) to area (e)) on one substrate.

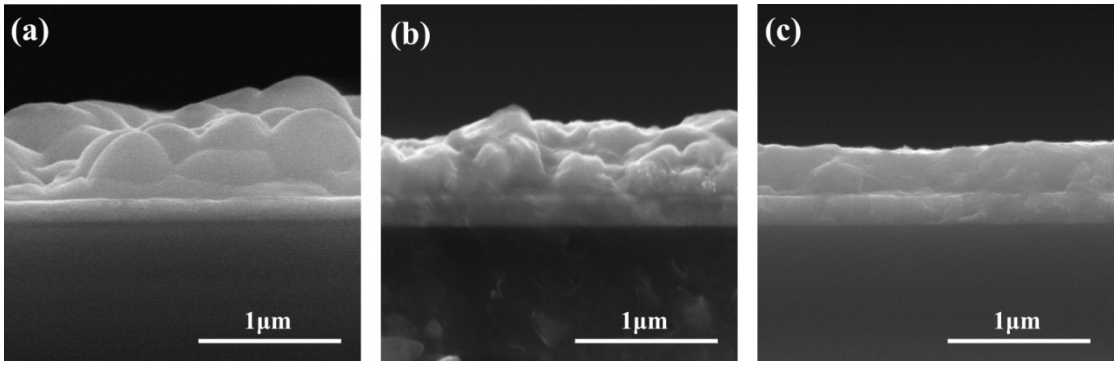

Fig. S5 Cross-sectional SEM images of perovskite films made by (a) sequential deposition, (b) one-step deposition and (c) MAD.

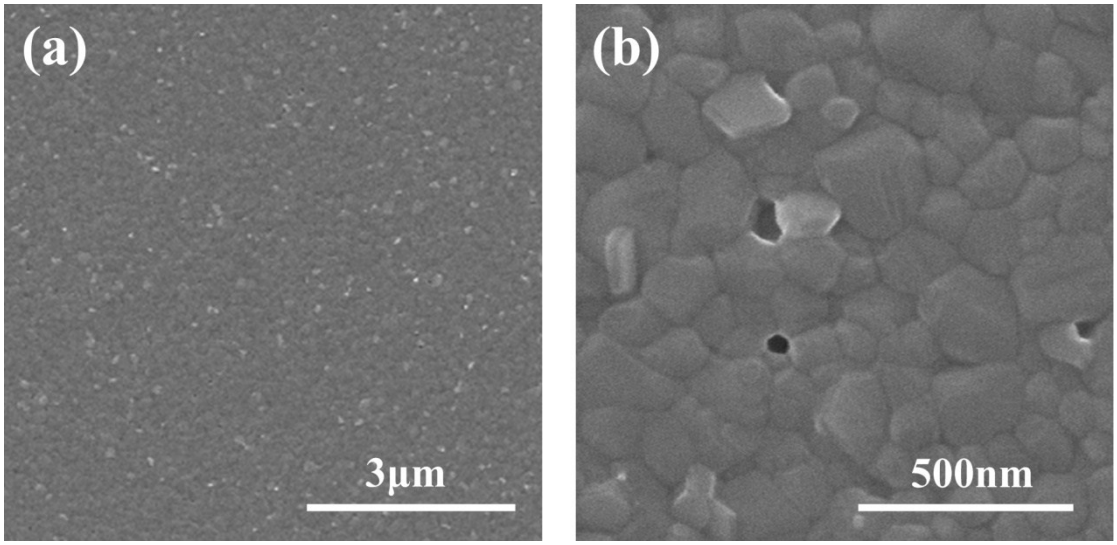

Fig. S6 Large and small magnitude SEM images of perovskite films prepared under a low speed N_2 flow of 400 L h^{-1}.

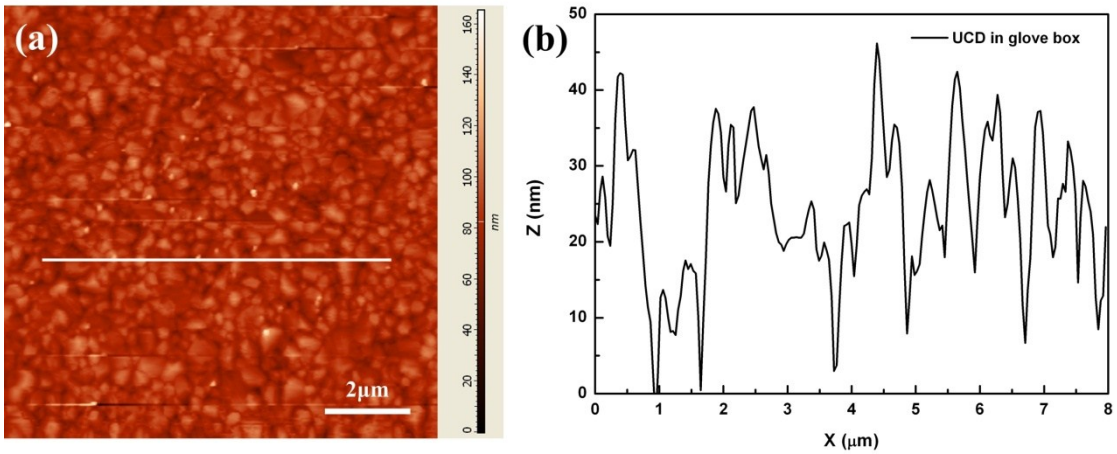

Fig. S7 AFM images and RMS analyses of perovskite films prepared in N_2-filled glove box with only chlorobenzene and without N_2 blow.

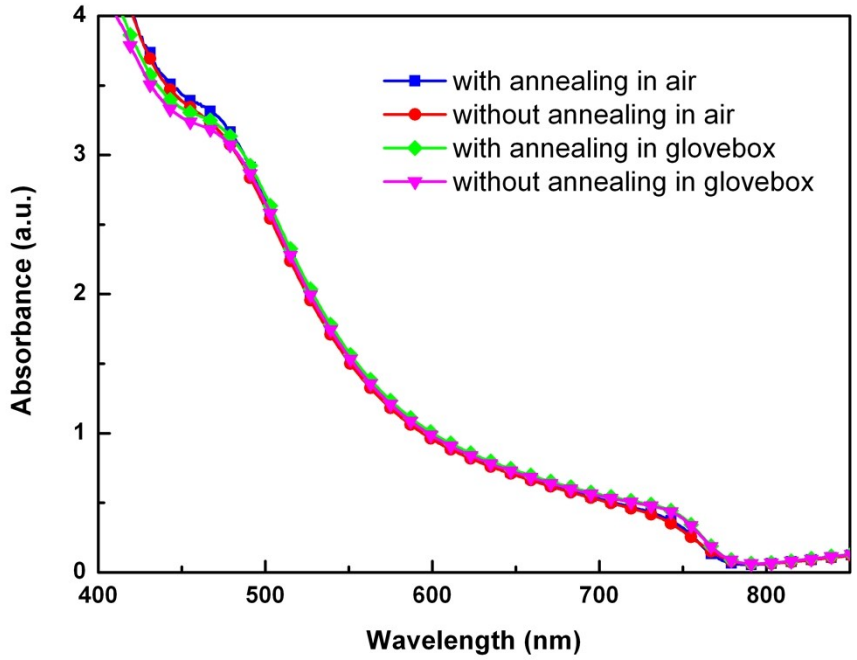

Fig. S8 Absorption spectra of perovskite films prepared by MAD in different environment conditions with and without annealing process.

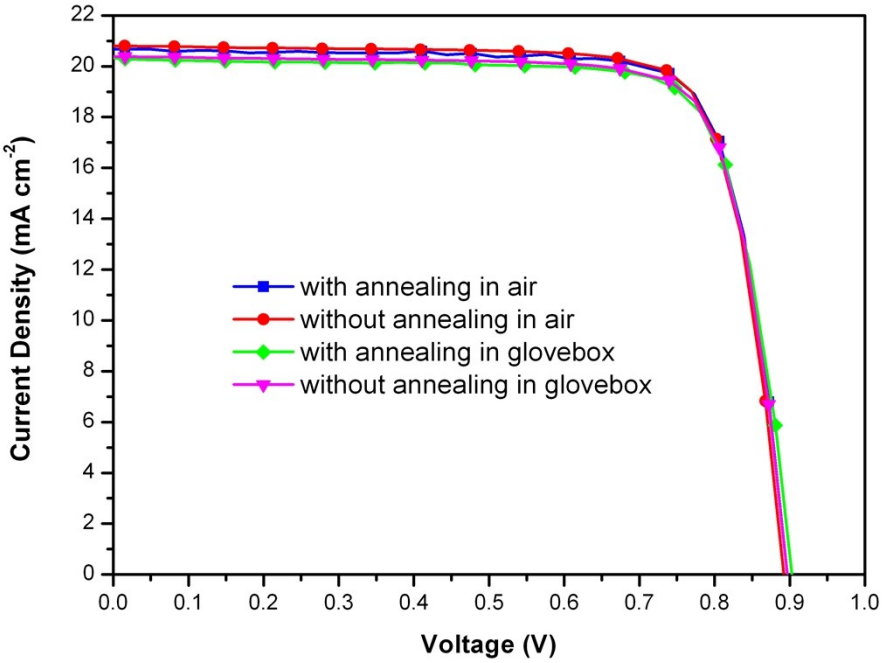

Fig. S9 Photovoltaic performance of devices with perovskite films prepared by MAD in different environment conditions with and without annealing process.

Table S1 Photovoltaic performance of devices with perovskite films prepared by MAD in different environment conditions with and without annealing process.

Devices	J_{sc} (mA cm^{-2})	V_{oc} (V)	FF (%)	PCE (%)
with annealing in air	20.68	0.89	79.2	14.58
without annealing in air	20.80	0.89	79.0	14.63
with annealing in glovebox	20.38	0.89	79.4	14.41
without annealing in glovebox	20.32	0.90	78.3	14.32

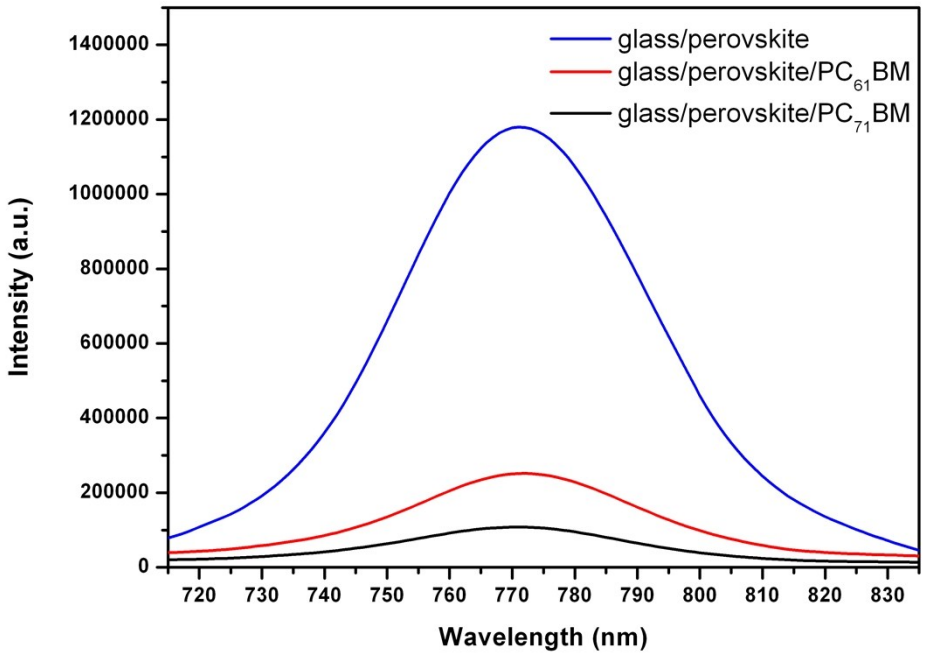

Fig. S10 PL quenching for perovskite films with different electron transport layers.

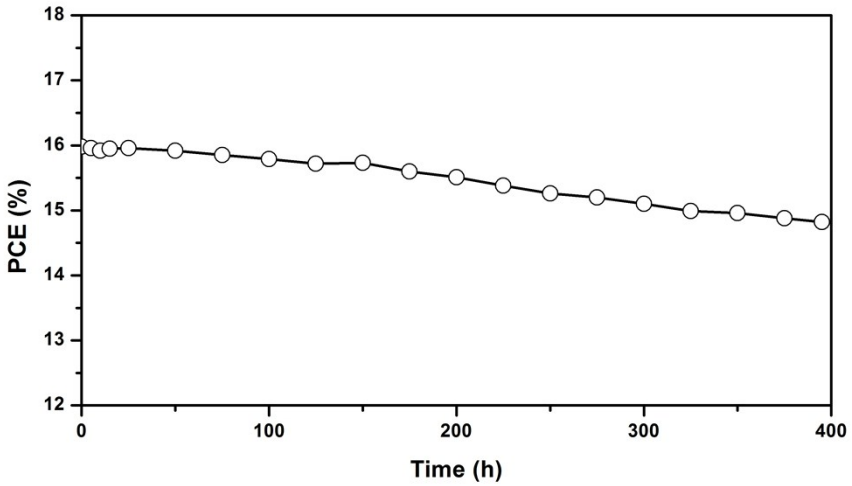

Fig. S11 Stability of devices prepared by MAD in ambient condition without encapsulation.